Integrating the controlled evaporation mixer with cavity ring-down spectroscopy for enhanced water vapor isotope calibration

Jangil Moon[1], Yeongcheol Han[1*] , Songyi Kim[1,2], Jeonghoon Lee[2] and Soon Do Hur[1]

Abstract

Accurate measurement of water vapor isotopes ($\delta^{18}O$ and δ^2H) is fundamental for advancing our understanding of the hydrological cycle and improving hydrological model accuracy. This study introduces an innovative calibration methodology using a controlled evaporation mixer (CEM) for determining stable isotopic ratios in atmospheric water vapor via cavity ring-down spectroscopy. The CEM technique reliably produces a stable water vapor stream, crucial for enhancing the precision and accuracy of isotopic measurements. Its rapid adaptation to changes in water vapor concentration and compatibility with different water standards enhance calibration reliability. Demonstrated reproducibility in generating water vapor across a broad concentration range from 900 to over 25,000 ppmv, coupled with a substantial reduction in memory effects, makes this approach highly effective in both laboratory and field settings. This calibration advancement greatly enhances research capabilities for continuous atmospheric water vapor analysis, providing deeper insights into hydrological processes and atmospheric dynamics.

Keywords Isotope calibration, Water vapor isotopes, Stable isotopes, CRDS, Vaporization

Introduction

Water stable isotopes ($\delta^{18}O$ and δ^2H) play a crucial role in unraveling the complexities of the Earth's water cycle, providing insights that have greatly enhanced our understanding of hydrological processes (Dansgaard 1964; Gat 1996; Galewsky et al. 2016). Although research on the isotopic compositions of liquid water and ice has progressed considerably, the exploration of water vapor isotopes has not been as extensive (Noone 2012; Griffis 2013; Galewsky et al. 2016). This gap presents a unique opportunity to deepen our knowledge of hydrological phenomena, particularly the transitions among vapor, liquid, and ice phases, and to enhance the predictive capabilities of hydrological models (Craig and Gordon 1965; Risi et al. 2010; Galewsky et al. 2016; Graf et al. 2019).

Traditionally, water vapor isotope analysis relied on cryogenic trapping, which necessitated prolonged collection periods and the use of freezing agents to accumulate sufficient volumes of condensed liquid for analysis (Schoch-Fischer et al. 1983; Helliker et al. 2002; Strong et al. 2007; Kim et al. 2016). While effective, this method required very careful handling to prevent isotopic fractionation during multiple phase transitions in sample collection, posing significant challenges in maintaining data accuracy, particularly in dynamic hydrological processes. Samples collected using the cryogenic method can be analyzed with comparable precision using isotope ratio mass spectrometry (IRMS) or cavity ring-down spectroscopy (CRDS) (Kim et al. 2016). Nonetheless, the advent of CRDS has notably transformed this field by enabling continuous and rapid measurements that directly assess the isotopic composition of water vapor without the need for phase changes (Gupta et al. 2009).

---

*Correspondence:
Yeongcheol Han
yhan@kopri.re.kr
[1] Korea Polar Research Institute, Incheon 21990, Korea
[2] Ewha Womans University, Seoul 03760, Korea

CRDS technology introduces a constant sample flow into an optical cavity, where the absorption of laser light by water vapor alters the ring-down times at various wavelengths, each corresponding to specific isotopologues. This technique allows for the immediate and precise determination of the isotopic compositions, thereby eliminating the need for labor-intensive requirements of previous methods. Furthermore, the portability and ease of CRDS setups have enabled on-site measurements across varied environmental conditions, greatly widening the research scope and improving understanding of moisture dynamics in different climates (Gupta et al. 2009; Bailey et al. 2015; Bonne et al. 2019; Lee et al. 2020).

Given that the ring-down times within the cavity are affected by both humidity and its isotopic composition, there is a risk that humidity fluctuations might be misconstrued as isotopic variations (Gupta et al. 2009). This issue is compounded by the fact that CRDS responses can vary across different instruments and over time, particularly in environments with low ambient humidity, where small changes in moisture levels can significantly impact isotopic readings (Tremoy et al. 2011; Casado et al. 2016; Weng et al. 2020). Such variations highlight the need for robust calibration methods that accurately distinguish between actual isotopic changes and those induced by shifts in humidity levels (Tremoy et al. 2011).

To address these challenges, calibration procedures involve injecting a water vapor stream with a known isotopic composition into CRDS equipment at various concentration levels to monitor the instrument's response and apply humidity dependency corrections to the analysis results. To achieve this, water vapors are typically generated by vaporizing liquids with known isotopic compositions, and various designs have been developed for this purpose. The most typical method involves vaporization at high temperatures, ranging from commercial products (Steen-Larsen et al. 2013; Weng et al. 2020) to custom-made setups (Gkinis et al. 2010; Zannoni et al. 2019). Other approaches have also been developed that utilize evaporation of liquids at relatively lower temperatures under dry conditions, such as the bubbler method (Wen et al. 2012; Steen-Larsen et al. 2014; Bailey et al. 2015), and the undersaturated evaporation of microdrops (Casado et al. 2016; Leroy-Dos Santos et al. 2021). Depending on the research purpose, these calibration methods aim to cover a wide range of water vapor concentrations, from as low as 100 ppmv for measurements in low-humidity environments like polar inlands (Leroy-Dos Santos et al. 2021) to up to 30,000 ppmv in the marine boundary layer (Steen-Larsen et al. 2014).

In addition to the previous efforts for calibration, this study introduces an innovative procedure using a controlled evaporation mixer (CEM), which ensures a consistent water vapor flow at desired concentrations. By utilizing two liquid standards with different isotope compositions and finely adjusting the flow rates of vaporizing liquid water and carrier gas, this system achieves precise calibration of CRDS instruments across a broad range of water vapor concentrations. This method enhances the accuracy and reliability of water vapor isotopic analysis in both laboratory and field settings. Through this advancement, we aim to enhance the precision of isotopic measurements, contributing to a more nuanced understanding of hydrological systems and potentially improving the predictive accuracy of hydrological models.

Method

Calibration system design

A calibration system was designed to produce a consistent flow of water vapor at desired concentrations. The schematic representation of this system is depicted in Fig. 1. This system utilized a CEM (Model W-102A, Bronkhorst, Netherlands), integrating a three-way mixing valve and an evaporator. The mixing valve enabled the creation of a mixture comprising liquid water and a carrier gas (either dry compressed air or synthetic zero air with 79% N_2 and 21% O_2). The evaporator ensured complete vaporization of this mixture at a set temperature (110 °C). Liquid flow was precisely regulated by the CEM, based on feedback from a Coriolis liquid flow meter (Model M12), ensuring accurate mixture composition. A stable flow of the carrier gas was maintained using a mass flow controller (Model F-201CV), crucial for consistent water vapor concentrations. The flow rates were separately controlled by a control unit (Model E-8303) and managed through software provided by the manufacturer.

Standard materials

In this study, two water types with distinct isotope compositions were used as working standards: de-ionized laboratory tap water (MQ; $\delta^{18}O = -8‰$, $\delta^2H = -56‰$) and commercial bottled water (BW; $\delta^{18}O = -14‰$, $\delta^2H = -99‰$). Each water was prepared in a 20 L container and aliquoted to a 150 mL stainless-steel cylinder of the CEM (Fig. 1). To address potential changes in the isotopic composition of the working standards, ∼5 mL of the standard waters in the cylinders was periodically extracted for liquid analysis on the VSMOW-SLAP scale. Over a month, changes in isotopic composition were negligible compared to the initial composition determined from the water in the 20 L container, with standard deviations of 0.08‰ for $\delta^{18}O$ and 0.9‰ for δ^2H (n = 10), which are comparable to the inherent precision of the instrument.
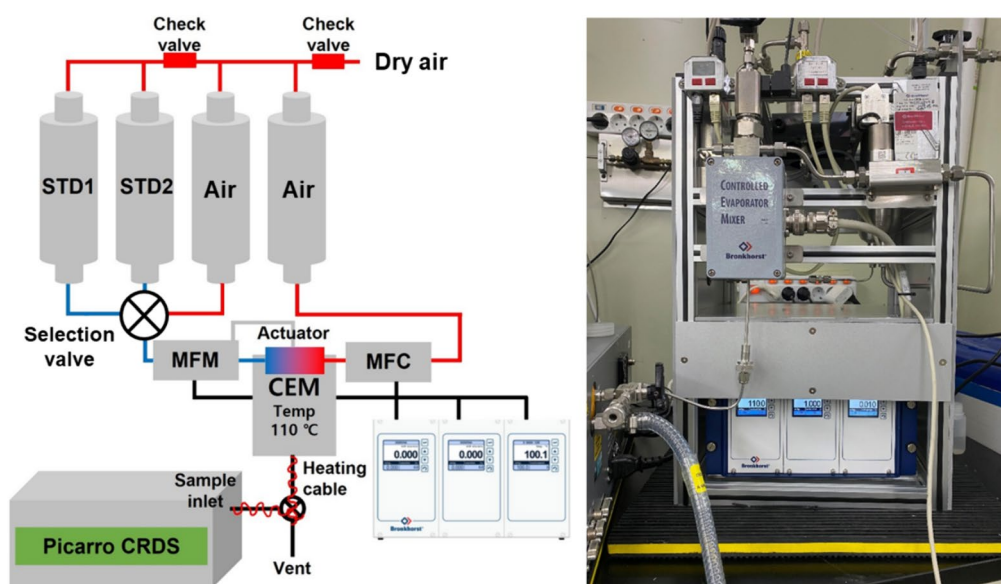
Fig. 1 Schematic diagram and photograph of the calibration system. The system includes a controlled evaporation mixer (CEM) set at 110 °C, connected to a selection valve for selecting between two standard water types (STD1 and STD2) and dry air. The mass flow controller (MFC) ensures precise regulation of carrier gas flow rates. A heated sample inlet line directs the mixed vapor to the CRDS for isotopic analysis, with the option to vent excess gas. Check valves are in place to prevent backflow, and the actuator controls the operation of the CEM

A selection valve facilitated the switching between water sources during calibration. Water delivery to the CEM was achieved by pressurizing the cylinders using either carrier gas from an ambient air compressor or a high-pressure gas source, such as a zero air compressed gas cylinder. The performance was reliable across all tests irrespective of pressure source, with a focus on using the ambient air compressor for consistency. The carrier gas was dehumidified below 50 ppmv using drierite cylinders.

Water vapor generation and performance evaluation
Our goal was to generate water vapor within a concentration range from 900 to over 20,000 ppmv. We adjusted the flow rates of the vaporizing liquid water and the carrier gas to achieve this. The carrier gas flow rate was set at 2 L per minute (L min^{-1}), while the flow rates of the liquid standards were systematically varied. This method was preferred over alternatives, such as keeping the liquid volume constant while adjusting the carrier gas flow rate or altering both flow rates simultaneously, to ensure uniformity in the total flow of the resulting vapor–gas mixture.

The performance of the calibration system was evaluated using a L2130-i cavity ring-down spectrometer (Picarro Inc., USA). In the analyzer, maintaining a low-pressure condition inside the optical cavity facilitated the introduction of the sample gas. The system consistently maintained cavity pressure and temperature at 50 Torr and 80 °C, respectively, through an integrated operation of a diaphragm vacuum pump, a position-controlled valve, and a heating module. This setup enabled a steady flow rate of approximately 40 standard cubic centimeters per minute (sccm), allowing for precise and reliable isotope analysis.

The performance of the system, encompassing consistent water vapor generation and analytical precision across various concentration ranges, was assessed through standard deviations (SDs) of water concentration, $\delta^{18}O$, and δ^2H values generated by the spectrometer. Measurements were conducted at the default data acquisition frequency of 1.2 Hz, equivalent to every 0.85 s, extending over 100 min for each targeted concentration level within 900–20,000 ppmv using both MQ and BW as test samples.

To examine the adaptability of the system and its control over memory effects, we observed the time it took for the system to reach equilibrium following step changes in water vapor concentration. Additionally, the return of water vapor concentrations to baseline levels was monitored after introducing dry compressed air into the system. We continuously monitored isotopic values as the water vapor concentration was systematically reduced from 8000 to 1000 ppmv and then raised back to 8000 ppmv, with each step change of 1000 ppmv occurring at 10-min intervals. This procedure enabled us to observe the hysteresis of isotopic signatures in response to these concentration changes.

Field testing

In a practical application of the CEM system, a case study was conducted in May 2023 at the Korea Polar Research Institute (KOPRI) in Incheon, Korea. The entire setup was installed next to a window approximately 15 m above ground level, with inlet Teflon tubing of less than 1 m in length equipped with a 0.2 μm in-line filter, heated to 60 °C to prevent water vapor condensation, and regulated at a flow rate of 1 L min^{-1}. Calibration using the CEM was performed before and after atmospheric sampling at three humidity levels between 10,000 and 25,000 ppmv, taking into account the humidity of the external sample air.

Results and discussion

Stability and precision of water vapor generation and isotopic measurements

Figure 2a illustrates the analysis of water vapor concentrations at 900, 2000, 4000, 12,000, and 20,000 ppmv for both water types. Notably, the SDs were uniformly maintained at approximately 30 ppmv (± 5 ppmv, standard deviation of the SDs; n = 10) across the entire range of tested concentrations. This consistency in SDs across diverse concentration levels underscores the ability of the calibration device to deliver a highly stable water vapor stream to the CRDS over prolonged durations (>100 min), enabling precise calibration of water vapor isotope ratios without significant drift in performance.

The CRDS manufacturer offers a vaporizer (e.g., Model A2011, Picarro inc., USA) optimized for liquid water analysis that similarly employs vaporization to channel water vapor to the cavity through carrier gas. This method involves injecting a specific volume of liquid

water into a heated chamber for vaporization. While effective in generating desired water vapor concentrations, it faces limitations due to the chamber volume, which restricts continuous water vapor supply and necessitates additional apparatus for precise water injection. Furthermore, when altering the injected solutions—such as between different types of standards—the need to mitigate the memory effect arises, as it could potentially affect measurement accuracy through residues from prior injections.

The calibration system developed in this study presents significant advancements over the conventional vaporizer, particularly in achieving remarkable stability in water vapor generation over prolonged durations. It efficiently overcomes the limitations of chamber volume and simplifies the mitigation of memory effects (Sect. 3.2), thereby enabling an accurate calibration of isotope ratio.

As shown in Fig. 2b, incremental increases in water vapor concentrations were accompanied by reductions in the standard deviations (SDs) for isotopic measurements of $\delta^{18}O$ and $\delta^{2}H$. This inverse correlation implies enhanced measurement precision at higher water vapor concentrations, likely due to reduced instrumental uncertainty with more light-adsorbing water molecules present. The observed data support the functional effectiveness of the commercial Picarro vaporizer, designed to perform optimally at water vapor concentrations around 20,000 ppmv for discrete liquid sample analysis.

The precision for $\delta^{18}O$ measurements was better than that for $\delta^{2}H$, as illustrated in Fig. 2b, consistent with the spectrometer's specifications which indicate that $\delta^{2}H$ measurements typically exhibit 4–5 times greater variability than $\delta^{18}O$. This variance does not present a
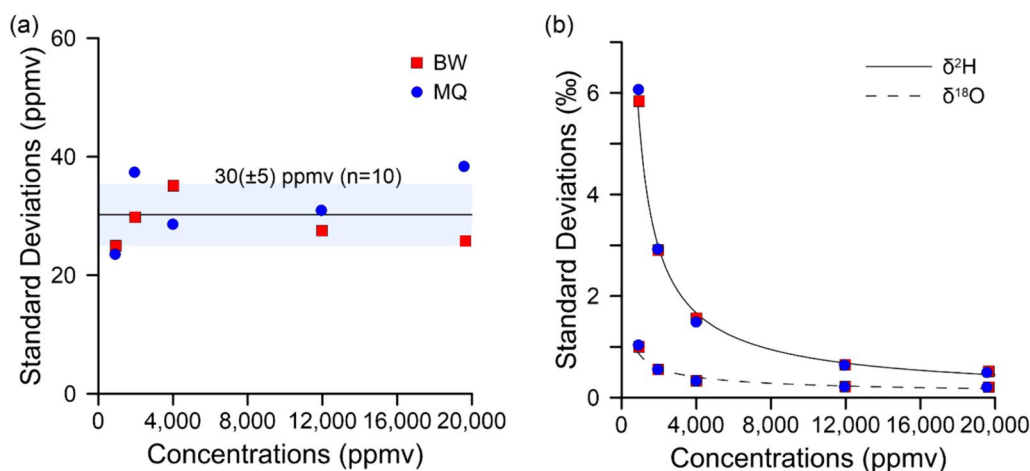
Fig. 2 Precision of isotopic measurements at varied vapor concentrations. **a** The standard deviations (30 ± 5 ppmv) for vapor concentration measurements of bottled water (BW) and de-ionized water (MQ) across various concentrations. **b** The precision of isotopic ratios represented by standard deviations for $\delta^{2}H$ (solid line) and $\delta^{18}O$ (dashed line) at each tested level

concern, given the naturally higher variability of δ^2H—about 8 times that of $\delta^{18}O$ in meteoric waters.

Consistency in analytical precision was maintained for both deionized water (MQ) and bottled water (BW), even with the higher dissolved solids content of BW. The minimal impact on isotopic measurement accuracy from differing sample compositions underscores the robustness and reliability of the analytical method.

To enhance the signal-to-noise ratio, the raw data collected at a frequency of 1.2 Hz was averaged over time. The resulting Allan deviation plots for $\delta^{18}O$ and δ^2H isotopic measurements, presented in Fig. 3, showed slopes near −0.5 on a log–log scale, indicating the predominance of flicker noise. The fluctuations observed at longer averaging times were likely due to the limited number of data points at these extended periods. Based on these findings, an optimal averaging time of 120 s was determined, corresponding to the integration of 140 data records, consistently achieving the desired precision—below 0.1‰ for $\delta^{18}O$ and 1‰ for δ^2H. The Allan deviation plots did not exhibit a plateau within the evaluated averaging times, suggesting no imminent transition to a different noise regime. This chosen integration time was determined strategically, as it offers the shortest analysis period that meets the precision criteria for the range of water vapor concentrations tested.

Response time and memory effect

During the calibration process, we assessed the response time to changes in water vapor production. Figure 4 documents a series of step decreases in water vapor concentration along with the corresponding stabilization times.
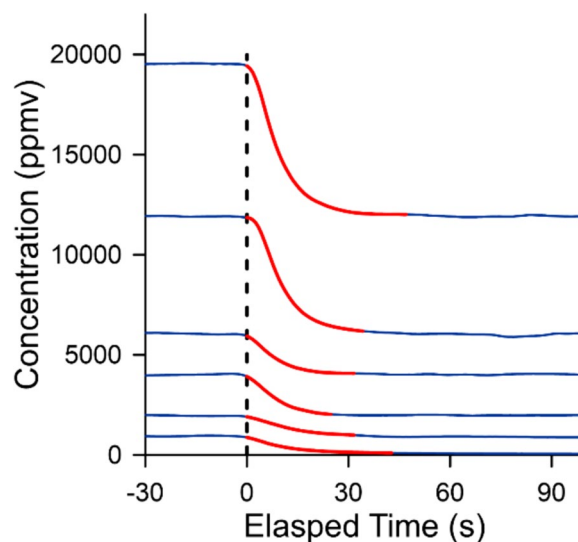
Fig. 4 Stabilization times (red lines) following step changes in vapor concentrations

The system consistently demonstrated a rapid response, with signals typically stabilizing within 60 s, reflecting its capacity for quick adaptation.

Upon reducing the water vapor concentration from 1000 ppmv to zero air, the concentration levels were observed to quickly drop below 100 ppmv within one minute and to under 50 ppmv shortly thereafter. This rapid decline signifies the effective management of memory effects, ensuring that isotopic signatures left from previous measurements are swiftly cleared to levels that do not interfere with subsequent analyses. Implementing
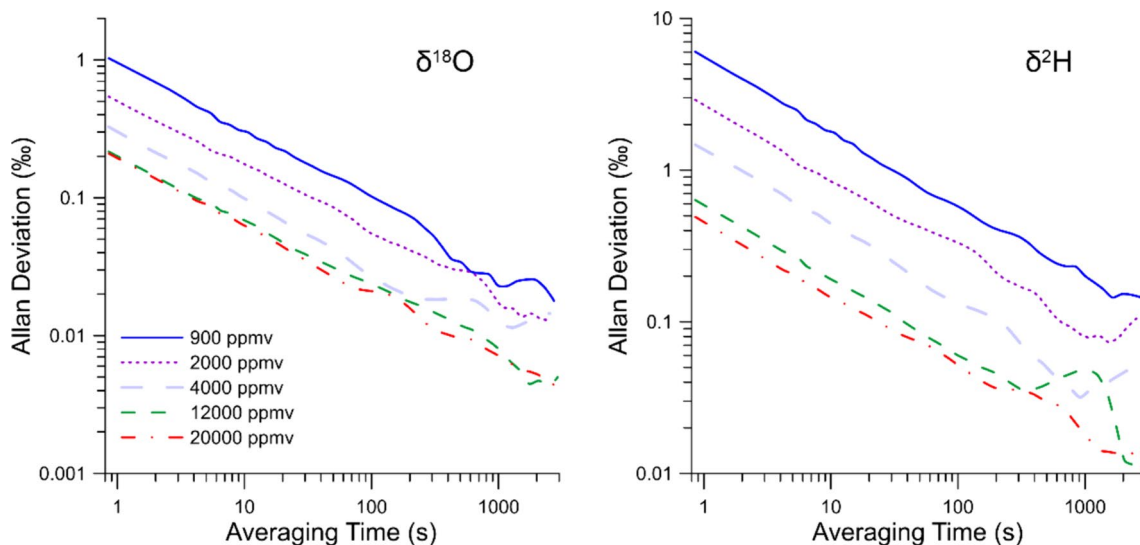
Fig. 3 Allan deviation plots for $\delta^{18}O$ (left) and δ^2H (right), illustrating measurement stability at different averaging times for selected vapor concentrations (900, 2000, 4000, 12,000, and 20,000 ppmv)

the procedure shown in Fig. 4, wherein subsequent analyses are performed in a descending concentration order, serves to further mitigate memory effects. For example, after analyzing MQ and drying the line to below 50 ppmv, introducing BW at 20,000 ppmv resulted in a negligible impact on $\delta^{18}O$ and δ^2H measurements. Any potential change in isotopic readings was limited to an increase of 0.02‰ for $\delta^{18}O$ and 0.10‰ for δ^2H, remaining well within the margin of analytical precision. This approach effectively reduces memory effects, thereby improving the reliability of the calibration process.

Memory effects, crucial to consider in water isotope analysis using CRDS, typically stem from isotopic signatures that linger on contact surfaces during sample transfer. Influenced significantly by sample purity and the interaction with elements like sample vials, autosampler syringes, and vaporization units during liquid sample analysis, such effects are less problematic in gaseous sample analysis. For ambient air samples introduced directly into the CRDS, the main strategy involves preventing condensation by adequately heating the water vapor path, minimizing contact surface interactions, and, consequently, reducing the potential for memory effects (Fig. 1).

In our analysis of the isotopic composition data from Fig. 5, we observed only a minimal hysteresis effect during cycles of water vapor concentration changes. Notably, even as water vapor concentration was methodically decreased from 8000 to 1000 ppmv and then increased back to 8000 ppmv, the $\delta^{18}O$ and δ^2H measurements remained consistent at each level throughout both the descent and ascent.
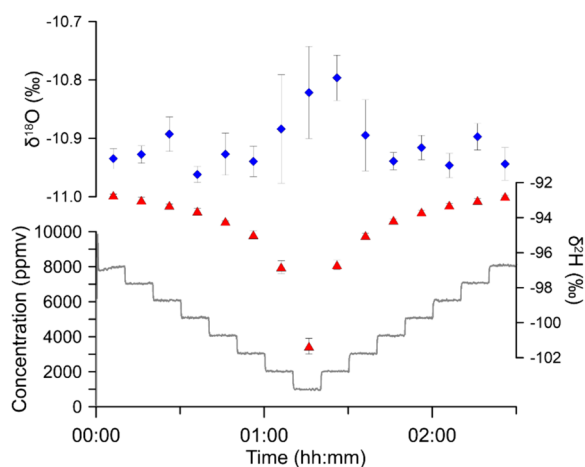

Fig. 5 Temporal variations in $\delta^{18}O$ (blue diamonds) and δ^2H (red triangles) isotopic ratios plotted alongside water vapor concentration (grey line) over a period, showing the system's hysteresis performance with minimal fluctuation in isotopic values during concentration cycling

The δ^2H values were more variable than those for $\delta^{18}O$, particularly at lower level (e.g., at 1000 ppmv), reflecting the increased dependency on water vapor concentration at lower levels (Fig. 5). Nevertheless, the δ^2H readings also exhibited a minimal hysteresis effect. The δ^2H readings presented a reliable and reproducible pattern as the water vapor concentrations changed, underscoring the dependable performance of the calibration system. Changes in $\delta^{18}O$ were nearly imperceptible, with any slight increases observed primarily at concentrations below 3000 ppmv, all falling within the stringent bounds of analytical precision. The consistency of these measurements, irrespective of the direction of concentration change, indicates that any memory effects are extremely limited and well within the acceptable parameters for analytical procedures.

Operation strategy for calibration
Building on the comprehensive analysis detailed in previous sections, we established an optimized calibration strategy for our analytical setup. The system first undergoes a rigorous purging process with dry air to achieve a low humidity baseline below 100 ppmv. Subsequently, a water standard—either MQ or BW—is introduced at predetermined concentrations. Our measurement protocol ensures that each specified water vapor concentration is maintained for at least three minutes, with a minimum of one minute dedicated to signal stabilization and two minutes for analysis. Prolonging this period can further enhance the precision. As delineated in Sect. 3.2, sequential analysis from higher to lower concentrations effectively mitigates memory effects. This cycle is repeated for the alternate standard. After analyzing each standard, the CEM and flow line are thoroughly purged with dry air, removing any residual moisture and preserving analytical integrity between standards.

Figure 6a demonstrates our calibrated approach, dedicating 10 min to each concentration level, starting with MQ followed by BW. The initial two minutes of data are omitted to prioritize the more stable data that follow, which are then segmented and integrated at two-minute intervals, yielding four distinct data points. Figure 6b, c aggregate these points to illustrate the mean values for $\delta^{18}O$ and δ^2H across a range of water vapor concentrations, elucidating the sensitivity of the isotope ratios to concentration changes. Both $\delta^{18}O$ and δ^2H exhibit decreasing trends with reduced water vapor concentrations, with the variation of δ^2H being more pronounced. These observations are consistent with previously documented studies (Bailey et al. 2015; Weng et al. 2020). According to Weng et al. (2020), this difference arises from lower natural abundance of HDO compared to $H_2^{18}O$ and increased sensitivity to changes in water vapor
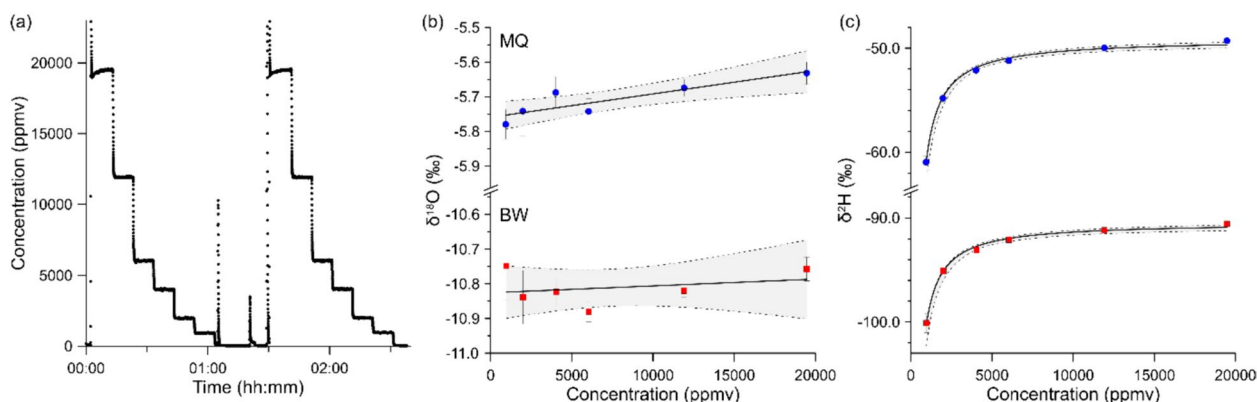
Fig. 6 **a** Vapor concentration profile during calibration steps. Respective best-fit curves for **b** δ^{18}O (linear) and **c** δ^2H (reciprocal) versus vapor concentrations

concentration, as well as a greater impact from isotopic fractionation. The δ^{18}O values show negligible fluctuation in response to changes in water concentration, indicating its stability under the studied conditions.

For calibration purposes, modeling the relationship between isotopic ratios and water vapor concentrations via curve fitting is vital. The relationship of δ^2H to concentration is effectively described by a reciprocal equation ($y = a + b/x$), while variation in δ^{18}O fits a simpler linear model ($y = a + bx$), despite a subtler correlation. The selection of a linear model for δ^{18}O is justified due to its minimal variability, with fluctuations confined to about 0.04‰ (RMSE) across the concentration spectrum. However, it is important to recognize that the influence of water vapor concentration on isotopic ratios can differ based on the equipment used, the isotopic composition of calibration standards, or over time. Hence, calibration needs may vary due to potential shifts in δ^{18}O and δ^2H responses to concentration changes under different instrumental conditions (Bailey et al. 2015; Weng et al. 2020). Ongoing monitoring and adaptation of the curve fitting to the most suitable model are essential to maintain the accuracy and integrity of isotopic ratio measurements. In line with these considerations, it is appropriate to tailor calibration interval and duration, concentration levels, and the types of standard materials according to the specific analysis conditions.

### Calibration of atmospheric water vapor measurements using CEM: a case study

The effectiveness of the CEM calibration system was demonstrated through a case study conducted at the KOPRI building. Calibration was performed at three different concentration levels, ranging from 10,000 to 25,000 ppmv, to cover a broad spectrum of atmospheric humidity conditions. Each concentration level was maintained and measured for six minutes, both before and after capturing the atmospheric data. This pre- and post-measurement calibration is crucial to account for any potential instrumental drift over time.

Figure 7 illustrates the calibration process. Initially, with a starting concentration of 10,000 ppmv, the CRDS response to different humidity levels was assessed by fitting the responses of MQ and BW to linear models (Figs. 6c and 7). These models enabled the calculation of instrumental responses at the actual water vapor concentrations recorded during atmospheric analysis. Calibration curves at each concentration level were established by aligning atmospheric analysis results with the VSMOW-SLAP scale. This alignment involved comparing the actual isotope compositions, obtained from long-term liquid measurements (Sect. 2.2), against the instrumental responses derived from the calibration curves for MQ and BW.

To ensure precise calibration, measurements were taken both before and after the atmospheric data collection, generating two sets of calibrated values for each data point. These values were then averaged, with weights assigned based on their respective measurement times, to mitigate any potential time-dependent instrumental drift. Figure 8 illustrates this process, showing the temporal distribution of isotopic measurements and the corresponding calibration adjustments.

Results from two calibration sessions conducted nine days apart provided additional insights into the characteristics and stability of the CRDS system. The variability in the humidity dependence slope, which could switch between positive and negative, reflected the system's dynamic response to different conditions. Notably, greater variability was observed with BW compared to MQ, indicating that instrumental drift not only varies over time but also depends on the isotopic composition
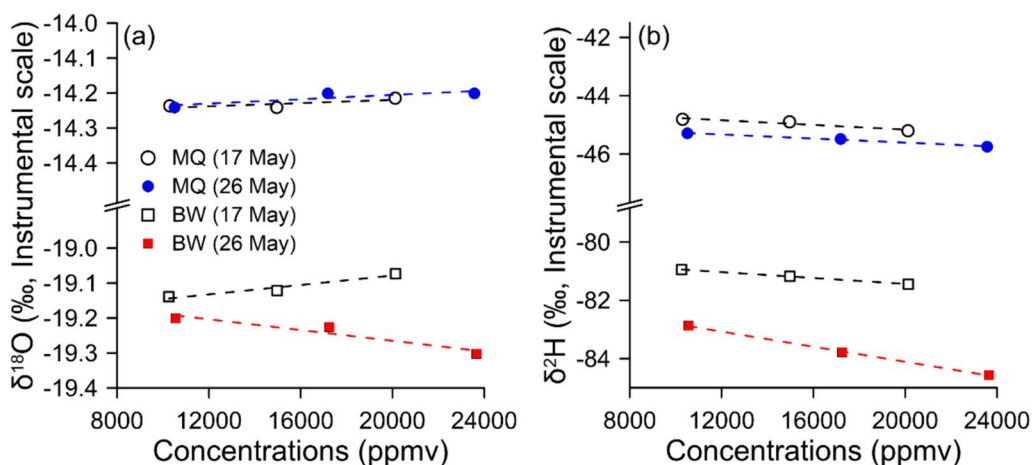
Fig. 7 Instrumental responses for (a) $\delta^{18}O$ and (b) $\delta^{2}H$ across varying concentrations on the instrumental scale. Open symbols represent water standard measurements taken on May 17, and solid symbols denote measurements on May 26 in 2023
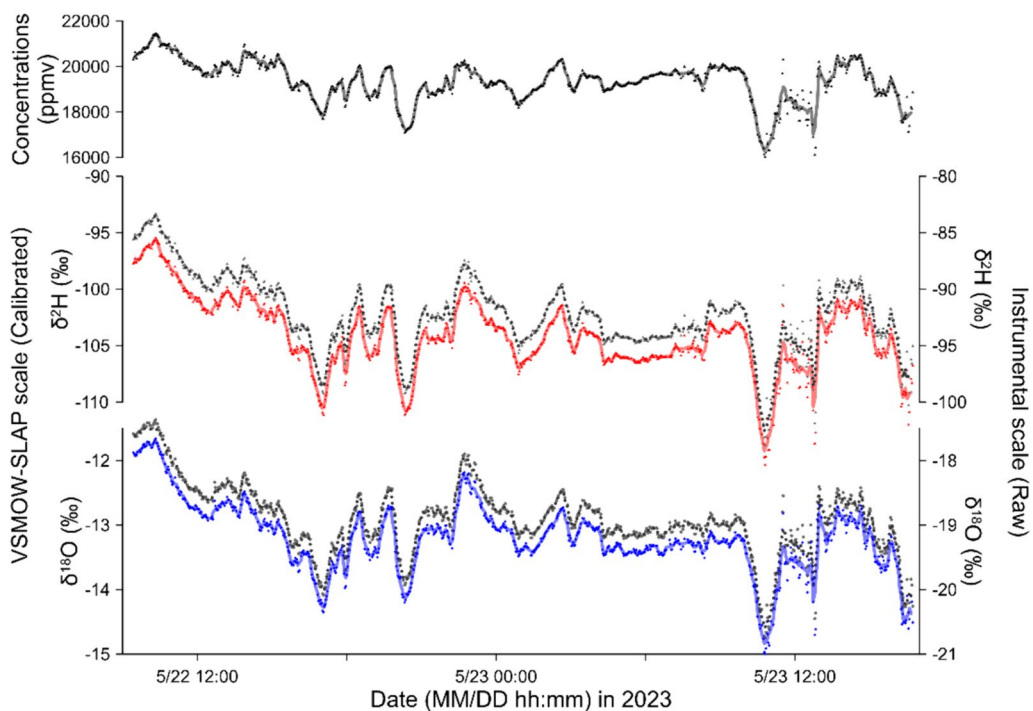
Fig. 8 Calibration results of atmospheric water vapor isotopic composition using the CEM system. Raw $\delta^{18}O$ and $\delta^{2}H$ values are presented in dashed black lines, with calibrated values adjusted to the VSMOW-SLAP scale shown in solid blue ($\delta^{18}O$) and solid red ($\delta^{2}H$) lines. All lines represent 10-min running averages. The calibration process included corrections for humidity dependency and instrumental drift

of the standard water. Despite these variations, the instrumental drift was confined within acceptable limits, with $\delta^{18}O$ variations limited to 0.2‰ and $\delta^{2}H$ variations to 2‰. This demonstrates the robust long-term stability of the system. Regular calibration, as demonstrated, effectively manages this level of drift, ensuring consistent measurement accuracy.

The CEM calibration method enhances the reliability of field measurements by providing a stable reference across various humidity levels, which is crucial in environments with fluctuating water vapor concentrations. By simulating different atmospheric moisture levels, compensating for instrumental drift, and adjusting the CRDS accordingly, the calibration method applied in the case study

ensures accurate isotopic measurements reflective of true atmospheric conditions.

Conclusions

This investigation has successfully developed a calibration technique for CRDS that enhances the precision of water vapor isotopic analysis. Utilizing a controlled evaporation mixer, this technique ensures consistent water vapor flow and accurate calibration over a wide range of concentrations, effectively minimizing memory effects and stabilizing water vapor generation. While concentrations down to 900 ppmv were tested in this study, further dilution is possible by integrating an additional mass flow controller with carrier gas into the final stage of our setup. This modification allows for calibrations at even lower concentrations, making the system highly beneficial in environments such as polar regions where precise calibration at extremely low humidity levels is crucial. This technique provides a more reliable method for analyzing water vapor isotopes, supporting future atmospheric water vapor studies to enhance our understanding of the hydrological cycle and improves hydrological forecasting accuracy.

Declarations

Competing interests
The authors declare that they have no competing interests.

References
Bailey A, Noone D, Berkelhammer M, Steen-Larsen HC, Sato P. The stability and calibration of water vapor isotope ratio measurements during long-term deployments. Atmos Meas Tech. 2015;8(10):4521–38.

Bonne J-L, Behrens M, Meyer H, Kipfstuhl S, Rabe B, Schönicke L, Steen-Larsen HC, Werner M. Resolving the controls of water vapour isotopes in the Atlantic sector. Nat Commun. 2019;10(1):1632.

Casado M, Landais A, Masson-Delmotte V, Genthon C, Kerstel E, Kassi S, Arnaud L, Picard G, Prie F, Cattani O, Steen-Larsen H-C, Vignon E, Cermak P. Continuous measurements of isotopic composition of water vapour on the East Antarctic Plateau. Atmos Chem Phys. 2016;16(13):8521–38.

Craig H, Gordon LI. Deuterium and oxygen 18 variations in the ocean and the marine atmosphere. In: Tongiorgi E, editor. Stable Isotopes in Oceanographic Studies and Paleotemperatures. Pisa: Consiglio Nazionale delle Ricerche, Laboratorio di Geologia Nucleare; 1965. p. 9–130.

Dansgaard W. Stable isotopes in precipitation. Tellus. 1964;16(4):436–68.

Galewsky J, Steen-Larsen HC, Field RD, Worden J, Risi C, Schneider M. Stable isotopes in atmospheric water vapor and applications to the hydrologic cycle. Rev Geophys. 2016;54(4):809–65.

Gat JR. Oxygen and hydrogen isotopes in the hydrologic cycle. Ann Rev Earth Planet Sci. 1996;24(1):225–62.

Gkinis V, Popp TJ, Johnsen SJ, Blunier T. A continuous stream flash evaporator for the calibration of an IR cavity ring-down spectrometer for the isotopic analysis of water. Isotopes Environ Health Stud. 2010;46(4):463–75.

Graf P, Wernli H, Pfahl S, Sodemann H. A new interpretative framework for below-cloud effects on stable water isotopes in vapour and rain. Atmos Chem Phys. 2019;19(2):747–65.

Griffis TJ. Tracing the flow of carbon dioxide and water vapor between the biosphere and atmosphere: a review of optical isotope techniques and their application. Agric for Meteorol. 2013;174–175:85–109.

Gupta P, Noone D, Galewsky J, Sweeney C, Vaughn BH. Demonstration of high-precision continuous measurements of water vapor isotopologues in laboratory and remote field deployments using wavelength-scanned cavity ring-down spectroscopy (WS-CRDS) technology. Rapid Commun Mass Spectrom. 2009;23(16):2534–42.

Helliker BR, Roden JS, Cook C, Ehleringer JR. A rapid and precise method for sampling and determining the oxygen isotope ratio of atmospheric water vapor. Rapid Commun Mass Spectrom. 2002;16(10):929–32.

Kim S, Han Y, Hur S-D, Lee J. Applications of cryogenic method to water vapor sampling from ambient air for isotopes analysis. Ocean Polar Res. 2016;38(4):339–45.

Lee D, Han Y, Kim S, Hur SD, Lee J. Development of a calibration system for stable water vapor isotope measurements using Cavity Ring-Down Spectroscope. J Geol Soc Korea. 2020;56(3):395–403.

Leroy-Dos Santos C, Casado M, Prié F, Jossoud O, Kerstel E, Farradèche M, Kassi S, Fourré E, Landais A. A dedicated robust instrument for water vapor generation at low humidity for use with a laser water isotope analyzer in cold and dry polar regions. Atmos Meas Techn. 2021;14(4):2907–18.

Noone D. Pairing measurements of the water vapor isotope ratio with humidity to deduce atmospheric moistening and dehydration in the tropical midtroposphere. J Clim. 2012;25(13):4476–94.

Risi C, Bony S, Vimeux F, Jouzel J. Water-stable isotopes in the LMDZ4 general circulation model: model evaluation for present-day and past climates and applications to climatic interpretations of tropical isotopic records. J Geophys Res Atmos. 2010;115(D12).

Schoch-Fischer H, Rozanski K, Jacob H, Sonntag C, Jouzel I, Östlund G, Geyh M. Hydrometeorological factors controlling the time variation of D, 18O and 3H in atmospheric water vapour and precipitation in the northern westwind belt. Isotope Hydrol. 1983;1984.

Steen-Larsen HC, Johnsen SJ, Masson-Delmotte V, Stenni B, Risi C, Sodemann H, Balslev-Clausen D, Blunier T, Dahl-Jensen D, Ellehøj MD, Falourd S, Grindsted A, Gkinis V, Jouzel J, Popp T, Sheldon S, Simonsen SB, Sjolte J, Steffensen JP, Sperlich P, Sveinbjörnsdóttir AE, Vinther BM, White JWC. Continuous monitoring of summer surface water vapor isotopic composition above the Greenland Ice Sheet. Atmos Chem Phys. 2013;13(9):4815–28.

Steen-Larsen HC, Sveinbjörnsdottir AE, Peters AJ, Masson-Delmotte V, Guishard MP, Hsiao G, Jouzel J, Noone D, Warren JK, White JWC. Climatic controls on water vapor deuterium excess in the marine boundary layer of the North Atlantic based on 500 days of in situ, continuous measurements. Atmos Chem Phys. 2014;14(15):7741–56.

Strong M, Sharp ZD, Gutzler DS. Diagnosing moisture transport using D/H ratios of water vapor. Geophys Res Lett. 2007;34(3).

Tremoy G, Vimeux F, Cattani O, Mayaki S, Souley I, Favreau G. Measurements of water vapor isotope ratios with wavelength-scanned cavity ring-down spectroscopy technology: new insights and important caveats for deuterium excess measurements in tropical areas in comparison with isotope-ratio mass spectrometry. Rapid Commun Mass Spectrom. 2011;25(23):3469–80.

Moon *et al. Journal of Analytical Science and Technology*   (2024) 15:42

Page 10 of 10

Wen X-F, Lee X, Sun X-M, Wang J-L, Tang Y-K, Li S-G, Yu G-R. Intercomparison of four commercial analyzers for water vapor isotope measurement. J Atmos Ocean Technol. 2012;29(2):235–47.

Weng Y, Touzeau A, Sodemann H. Correcting the impact of the isotope composition on the mixing ratio dependency of water vapour isotope measurements with cavity ring-down spectrometers. Atmos Meas Tech. 2020;13(6):3167–90.

Zannoni D, Steen-Larsen HC, Stenni B, Dreossi G, Rampazzo G. Synoptic to mesoscale processes affecting the water vapor isotopic daily cycle over a coastal lagoon. Atmos Environ. 2019;197:118–30.

Publisher's Note